W-band TE102-mode filter with doubly loaded E-plane and H-plane irises

Chad Bartlett[✉] and Michael Höft
Institute of Electrical and Information Technology, Chair of Microwave Engineering, University of Kiel, Kiel, 24143, Germany
[✉]Email: chb@tf.uni-kiel.de

In this correspondence, high-precision computer numerical control milling is utilised to demonstrate a doubly loaded iris, cross-coupled waveguide bandpass filter for inline operation within the W-band. This sixth-order filter is designed in a stacked H-plane configuration and utilises both E-plane and H-plane doubly loaded irises to maintain the flow of a TE102-mode electromagnetic field. In this configuration, a high rejection level is maintained outside of the passband while a good unloaded quality factor is obtained through the support of larger resonator dimensions. The filter is designed for approximately 2% fractional bandwidth centred at 97.5 GHz and has been fabricated as three brass components. Measurements of the filter agree very well with the simulated results and demonstrate a spurious-free design over the full W-band.

Introduction: As technology progresses within the communication, radar, and satellite industries, high-frequency designs require continuous adaptation and refinement to meet stringent specifications. An example of this type of constraint is the high selectivity required from filters that are placed between low-noise amplifiers and high-power amplifiers on satellite systems [1]. Naturally, the trade-off for high-frequency designs is the overall size and weight of RF components. This trade-off can be exploited for compact and lightweight components when employed appropriately but inversely comes at the cost of requiring high-precision manufacturing capabilities. In regards to W-band filters, only a few computer numerical control (CNC) milled designs have been demonstrated in the literature with elliptical/quasi-elliptical response [2–11], many of which rely on the use of source-load coupling techniques for the generation of additional transmission zeros but can go on to require bulky corner transitions. In this letter, we demonstrate an inline full-wave sixth-order quasi-elliptical filter with approximately 2% fractional bandwidth centred around 97.5 GHz by utilising symmetric E-plane and H-plane doubly loaded irises. In general, the complexity and fine detail of such attributes are difficult to achieve with standard CNC milling, but through the use of state-of-the-art high-precision CNC milling, the stringent dimensions are achieved and exhibit exceptional measured results. In addition, the filter structure remains compact and is able to maintain a spurious-free rejection of better than 30 dB between 75–95 GHz and 100–110 GHz while attaining a good unloaded quality factor.

Filter structure design: For the design of the filter, TE102-mode resonators are chosen and utilised in a stacked H-plane configuration. The TE102-mode resonators have been selected for their increased dimensions to ease milling as well as for their increased Q-factor capacity. In order to control the flow of the TE102 electromagnetic field, as well as maintain the structural symmetry of the input/output waveguides, doubly loaded irises are selected at several locations within the filter. As shown in Figure 1, the cross-coupling between resonators 1 and 6 takes the form of dual circular E-plane irises, and the main-line coupling paths between resonators 1 and 2 (and by symmetry, resonators 5 and 6) take the form of dual H-plane irises. Single irises are used for each of the remaining main-line couplings, where notably, a large single circular iris is used in the main-line coupling between resonators 3 and 4. A perspective view of the filter's vacuum shell, the electrical topology, and an outline of the given dimensions are described in Figure 1. Additionally, Figure 2 depicts the electromagnetic field interaction throughout the structure at 97.5 GHz. From this image, it is clear how the TE102 mode is passed through the dual H-plane irises between resonators 1 and 2. The generalised coupling matrix synthesis equations provided by [12] can be applied to describe the circuit, where the dual irises, in this case, are simply treated as single irises. The generalised coupling matrix profile can be described by

$$\begin{bmatrix} 0 & 1.020 & 0 & 0 & 0 & 0 & 0 & 0 \\ 1.020 & 0 & 0.856 & 0 & 0 & 0 & -0.070 & 0 \\ 0 & 0.856 & 0 & 0.610 & 0 & 0 & 0 & 0 \\ 0 & 0 & 0.610 & 0 & 0.614 & 0 & 0 & 0 \\ 0 & 0 & 0 & 0.614 & 0 & 0.610 & 0 & 0 \\ 0 & 0 & 0 & 0 & 0.610 & 0 & 0.856 & 0 \\ 0 & -0.070 & 0 & 0 & 0 & 0.856 & 0 & 1.020 \\ 0 & 0 & 0 & 0 & 0 & 0 & 1.020 & 0 \end{bmatrix}. \quad (1)$$

A comparison between the lossless simulated structure and the coupling matrix profile from Equation (1) is depicted in Figure 3 over the 93–102 GHz range.

Manufacture and measurements: The filter has been manufactured by a high-precision CNC milling process as three individual components.

The top and bottom components accommodate the six resonators while a thin foil of 0.1 mm thickness is placed between the top and bottom pieces in order to house the circular main-line and cross-coupling irises. It is clear that the size and position of the circular coupling irises placed within the thin foil are critical during manufacture as well as during the final filter assembly; metal alignment pins are used for the

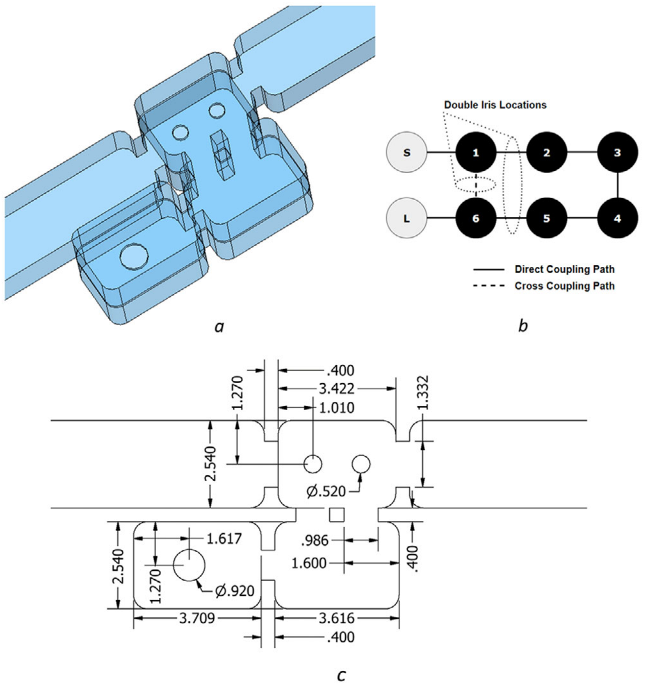

Fig 1 *Configuration of the TE102-mode filter (a) perspective view of the filter's vacuum shell, (b) cross-coupled filter topology, (c) basic filter dimensions in (mm)*

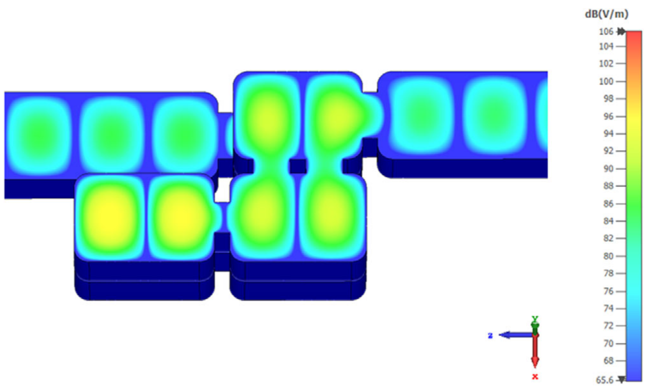

Fig 2 *Electromagnetic interaction of the TE102 mode throughout the filter (shown at 97.5 GHz)*

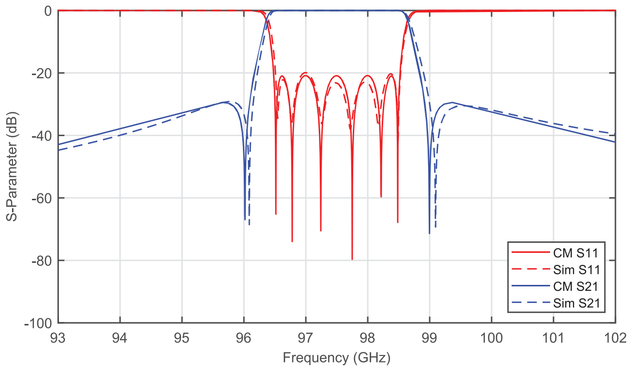

Fig 3 *Comparison of lossless simulated filter and coupling matrix profile from Equation (1)*

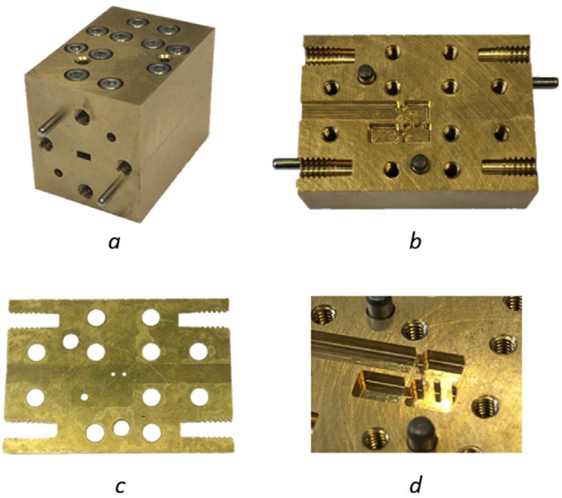

Fig 4 *Photos of the manufactured filter in brass (a) assembled filter, (b) top filter block housing three of the resonators, (c) foil section that houses the circular E-plane irises, (d) close-up view of a resonator section and an H-plane iris post*

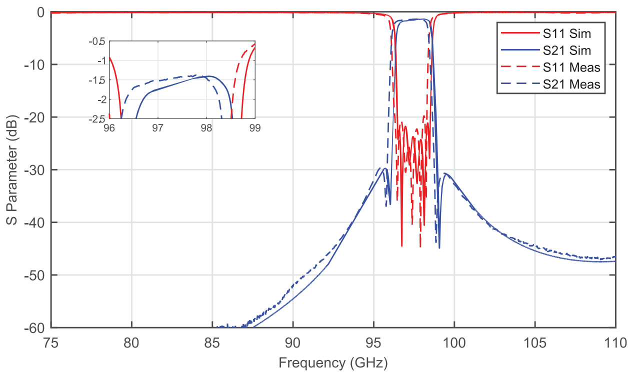

Fig 5 *Comparison of the lossy simulated filter and the measured results over the full W-band. The conductivity of brass is taken as 4.9e+06 S/m during simulation. Inset depicts a close-up view of the insertion loss*

precise positioning. Additionally, the size and position of the posts that separate the dual H-plane irises are critical, and care must be taken to achieve good electrical contact during assembly. Each of the three components has been manufactured in brass and the internal radii of corners are 0.4 mm. Figure 4 depicts images of the fully assembled filter, a milled resonator section, the thin foil, and a close-up view of the resonator section in order to highlight the H-plane iris post. The overall volume of the assembled filter is W × L × H = 20 × 28.22 × 22 mm.

The filter has been measured on a Rohde & Schwarz ZVA67 with W-band up-converters. A comparison of the simulated and measured response is shown in Figure 5 over the full frequency band of operation. It can be noted that good results are obtained in the passband as well as in both of the rejection regions with only a slight deviation from the centre frequency. The measured insertion loss of the passband reaches approximately 1.4 dB, while the return loss reaches the 20 dB level. The rejection region designated between 75–95 GHz and again at 100–110 GHz remains under 30 dB and spurious-free. The unloaded quality factor of this filter is calculated to be approximately $Q_u = 970$.

Although some of the losses can be attributed to the final-milled surface roughness, an additional source of degradation to the effective conductivity can come from any small misalignment or gaps between each of the three layers during the component assembly. To reduce some of these losses, a thin gold coating can be applied for better conductivity.

Conclusion: In this letter, we have presented a TE102-mode six-pole quasi-elliptical filter utilising doubly loaded E- and H-plane irises for operation at 97.5 GHz. The use of doubly loaded irises at the selected locations allows for simple and symmetric control over the flow of the TE102-mode electromagnetic field. High-precision milling has been employed to achieve the stringent dimensions required of these features. The measured results are in good agreement with the simulations and demonstrate a good unloaded quality factor for this frequency band. Additionally, a strong rejection level is maintained throughout the full frequency range without the use of additional transmissions zeros. This design demonstrates a feasible option for future high-frequency diplexer configurations as well as expanding on the concept of multi-loaded irises for the control of higher-order modes in complex geometries.

Acknowledgment: This project has received funding from the European Union's Horizon 2020 research and innovation programme under the Marie Skłodowska-Curie grant agreement 811232-H2020-MSCA- ITN-2018.

Author contributions: Conceptualization, data curation, formal analysis, investigation, methodology, and writing-original draft: Chad Bartlett. Funding acquisition, project administration, supervision, writing-review and editing: Michael Höft.

Received: *18 October 2020* Accepted: *16 November 2020*
doi: 10.1049/ell2.12003

References

1 Cameron, R. J., et al.: *Microwave Filters for Communication Systems: Fundamentals, Design and Applications*. Wiley, New York, NY, USA (2007)

2 Leal-Sevillano, C.A., et al.: Low-loss elliptical response filter at 100 GHz. *Microwave Wireless Compon. Lett.* **22**(9), 459–461 (2012)

3 Ding, J., et al.: W-band quasi-elliptical waveguide filter with cross-coupling and source–load coupling. *Electron. Lett.* **52**(23), 1960–1961 (2016)

4 Xu, J., et al.: W-band broadband waveguide filter based on H-plane offset coupling. *J. Infrared Millimeter Terahertz Waves* **40**(4), 412–418 (2019)

5 Xiao, Y., et al.: A novel W-band waveguide bandpass filter based on nonresonating nodes. In: IEEE International Conference on Microwave and Millimeter Wave Technology (ICMMT), vol. **2**, pp. 833–835.IEEE, Piscataway, New Jersey (2016)

6 Miek, D., et al.: Improved fully canonical phase equalized W-band waveguide filter with dispersive coupling inverter. In: 48th European Microwave Conference (EuMC), pp. 166–169.IEEE, Piscataway, New Jersey (2018)

7 Miek, D., et al.: Improved fully canonical W-band waveguide filter. In: IEEE MTT-S International Microwave Symposium Digest, Philadelphia, Pennsylvania, USA, pp. 1245–1248 (2018)

8 Miek, D., Höft, M.: Realization of folded W-band waveguide filters with additional asymmetric resonant transmission zeros. In: 12th German Microwave Conference (GeMiC), Stuttgart, Germany (2019)

9 Miek, D., et al.: Folded Wband waveguide filters with resonant coupling apertures for the generation of additional transmission zeros. *Frequenz* **73**(11-12), 379–388 (2019)
10 Arndt, F., et al.: Asymmetric iris coupled cavity filters with stopband poles. In: IEEE MTT-S International Microwave Symposium. Digest, Dallas, Texas, pp. 215–218 (1990)
11 Zhou, K., et al.: W-Band dual-band quasielliptical waveguide filter with flexibly allocated frequency and bandwidth ratios. *IEEE Microwave Wireless Compon. Lett.* **28**(3), 206–208 (2018)
12 Hong, J.-S., Lancaster, M.J.: *Microstrip Filters for RF/Microwave Applications*. John Wiley & Sons Inc., New York, NY, USA (2001)